PHYSICS OF FLUIDS **17**, 055110 (2005)

Two-equation modeling of turbulent rotating flows

J.-B. Cazalbou,[a] P. Chassaing,[b] G. Dufour, and X. Carbonneau
ENSICA, 1 Place Émile Blouin, 31056 Toulouse Cedex 5, France

(Received 31 October 2004; accepted 14 March 2005; published online 6 May 2005)

The possibility to take into account the effects of the Coriolis acceleration on turbulence is examined in the framework of two-equation eddy-viscosity models. General results on the physical consistency of such turbulence models are derived from a dynamical-system approach to situations of time-evolving homogeneous turbulence in a rotating frame. Application of this analysis to a (k,ϵ) model fitted with an existing Coriolis correction [J. H. G. Howard, S. V. Patankar, and R. M. Bordynuik, "Flow prediction in rotating ducts using Coriolis-modified turbulence models," ASME Trans. J. Fluids Eng. **102**, 456 (1980)] is performed. Full analytical solutions are given for the flow predicted with this model in the situation of homogeneously sheared turbulence subject to rotation. The existence of an unphysical phenomenon of blowup at finite time is demonstrated in some range of the rotation-to-shear ratio. A direct connection is made between the slope of the mean-velocity profile in the plane-channel flow with spanwise rotation, and a particular fixed point of the dynamical system in homogeneously sheared turbulence subject to rotation. The general analysis, and the understanding of typical inaccuracies and misbehavior observed with the existing model, are then used to design a new model which is free from the phenomenon of blowup at finite time and able to account for both of the main influences of rotation on turbulence: the inhibition of the spectral transfer to high wave numbers and the shear/Coriolis instability. © *2005 American Institute of Physics*. [DOI: 10.1063/1.1920630]

I. INTRODUCTION

When a turbulent flow undergoes system rotation, the resulting Coriolis accelerations are responsible for strong modifications to the statistical properties of the fluctuating field. The most spectacular ones are related to the shear/Coriolis instability,[1] the result of which may be either an enhancement ("destabilization") or a reduction ("stabilization") of the turbulent activity. The latter eventually leads to relaminarization. Both phenomena can be observed in radial turbomachines—especially small-size rotors operating at high rotation speed—with important consequences on the performance and efficiency of the stages. The mode of action of the shear/Coriolis instability can be understood within a statistical-description context: system rotation appears in the Reynolds-stress transport equations where it interacts with anisotropy in intercomponent-transfer terms. These terms are traceless—and therefore without contribution to the turbulent-kinetic-energy budget—but directly act on the shear stresses, which are either decreased or increased depending on the relative orientations of the system-rotation vector and Reynolds-stress tensor, hence the observed stabilization or destabilization processes. On the other hand, a second mode of action by which the Coriolis accelerations are known to modify the fluctuating field is not tractable within the context of one-point statistics: it affects the nonlinear spectral-transfer term of Lin's equation and leads to an inhibition of the energy cascade to small scales. As a result, reduction of the turbulent dissipation and simultaneous enhancement of the turbulent activity are observed.

From what precedes, it comes out that the origins of system-rotation effects on turbulence cannot be traced in the framework of one-point first-order turbulence modeling. Now, in an industrial context where the flow configurations are complex (three-dimensional geometries, relative motion between elements, inhomogeneity of the inlet conditions,…), it is important to mimic the effects of rotation with relatively simple turbulence models. This can be achieved by making model coefficients dependent on the rotation rate. With such an approach—a (k,ϵ) model and a simple modification proposed by Howard, Patankar, and Bordynuik[2]—Jongen, Machiels, and Gatski[3] have presented calculations of the plane-channel flow with spanwise rotation that are in excellent agreement with existing direct-numerical-simulation (DNS) results:[4,5] the computed flow exhibits stabilization (respectively, destabilization) in the vicinity of the suction (respectively, pressure) wall, a core region where the mean-velocity profile is linear with a slope close to twice the rotation rate (neutral-stability region), and accurate friction coefficients. Such a result obtained in a simple but representative flow configuration (stabilization and destabilization phenomena can be observed in the blade-to-blade channels of radial rotors) is encouraging. It motivates the present study that aims at developing calculation methods that are efficient in the prediction of rotating flows, and do not involve more than a marginal increase in the computational cost, as compared to the "industry standards." However, accurate prediction of the channel flow is a somewhat too restricted basis to validate a model of sufficiently general use. In order to widen this basis, two well-documented flow configurations are considered, in which the Coriolis accelerations directly

[a]Electronic mail: cazalbou@ensica.fr
[b]Also at INPT-ENSEEIHT-Institut de Mécanique des Fluides de Toulouse UMR 5502 CNRS, France.

influence the fluctuating field without affecting the mean flow. These are ordinary situations of time-evolving homogeneous turbulence undergoing rotation: initially isotropic turbulence and homogeneously sheared turbulence (further referred to as the HI-Ω and HS-Ω flows). In the first case, limited departures from isotropy of the Reynolds-stress tensor remove the shear/Coriolis-instability mechanism from the problem, and leave the nonlinear effect acting alone. In the second case, anisotropy is enforced by mean shear and the instability mechanism dominates. The model problems corresponding to these situations will be stated in Sec. II for two-equation eddy-viscosity models. They can be studied using a dynamical-system approach,[6] and it will be shown that the fixed-point diagram obtained in the sheared case must possess some precise properties in order to ensure physical consistency. Applying this analysis to the correction method of Howard, Patankar, and Bordynuik[2] in Sec. III will illustrate typical inaccuracies and unphysical behavior that can result when the diagram does not possess the desired properties. Based on these results, a new Coriolis correction is finally proposed in Sec. IV. Unlike earlier proposals, it accounts for both the nonlinear effects and the shear/Coriolis instability.

II. ROTATING HOMOGENEOUS TURBULENCE

We consider the flow of an incompressible fluid in a Cartesian coordinate system (x,y,z) rotating around the z axis with an angular velocity Ω relative to a Galilean reference frame. The turbulence Reynolds number is high and the statistical properties of the fluctuating field remain homogeneous in space at any time. The statistics evolve in time from an initial state at $t=0$ characterized by the levels k_0 and ϵ_0 of the turbulent kinetic energy k and dissipation rate ϵ. These assumptions apply to both of the HS-Ω and HI-Ω flows.

A. Homogeneously sheared turbulence

In this case the mean flow is unidirectional and the only nonzero element $S=\partial\overline{U}/\partial y$ of the velocity-gradient tensor is constant in time and space (U is the velocity component along x and the overbar denotes statistical averaging). Without any loss of generality, we shall consider that S is positive. In the absence of rotation, experiment[7–9] and simulation[10,11] indicate that the flow evolves toward an equilibrium state where the turbulent time scale (k/ϵ) locks on to the mean-flow time scale $1/S$. Their ratio $\alpha=\epsilon/(Sk)$ then becomes a constant (≈ 0.22), independent of the initial conditions and shear-rate level as soon as the latter is sufficiently high (the "high-shear class of flows" reviewed by Tavoularis and Karnik[9]). That is, the turbulent kinetic energy and dissipation rate continuously increase at the same rate. As mentioned in the Introduction, the addition of system rotation significantly alters the picture: examination of the Reynolds-stress transport equations led Johnston, Halleen and Lezius[12] to hypothesize that the flow should become stable (i.e., the velocity fluctuations decrease with time) for negative values of the ratio $\beta=\Omega/S$, and remain unstable otherwise. On the other hand, displaced-particle analysis[13] and stability analysis[14–16] indicate that flow is linearly stable when β is outside the range 0–0.5. This result leads to the definition of the Bradshaw–Richardson number[15]

$$\mathrm{BR} = -2\Omega/S \times (1 - 2\Omega/S) = 2\beta(2\beta - 1),$$

and a criterion according to which linear stability corresponds to positive values of BR. Physical results would help to evaluate more precisely the stability characteristics of the fully turbulent flow, they are unfortunately scarce: The large-eddy-simulation (LES) results at $\beta=0$, 0.25, and 0.5 of Bardina, Ferziger, and Rogallo[11] confirm that the flow is unstable in this range, and their results at $\beta=0.5$ seem to exhibit a neutral character. Rapid-distortion-theory (RDT) results by Bertoglio[17] go from $\beta\approx -0.44$ to 0.44 and, in the meantime, the computed flow goes from stable to unstable, neutral flow being apparently obtained for a value of β significantly lower than zero (about -0.2). In the absence of precise bounds for the unstable-flow range, we shall consider that it extends from a value of β slightly below zero up to 0.5.

1. Turbulence-model corrections for the shear/Coriolis instability

Existing proposals for taking into account the shear/Coriolis instability in the context of two-equation turbulence modeling have often been obtained from an analogy between rotation and curvature effects. The corrections of Howard, Patankar, and Bordynuik,[2] and Chen and Guo[18] correspond to the curvature correction introduced by Launder, Priddin, and Sharma.[19] The $C_{\epsilon 2}$ coefficient of the destruction term in the dissipation equation is made rotation dependent through some form B of the Bradshaw–Richardson number:

$$C_{\epsilon 2} = C^0_{\epsilon 2}(1 - C_{\mathrm{sc}}B),$$

where $C^0_{\epsilon 2}$ and C_{sc} are positive constants. The model of Chen and Guo, and the model denoted as "Model II" in Howard *et al.*, use the following expression of the Bradshaw–Richardson number:

$$B = -2\Omega(S - 2\Omega)k^2/\epsilon^2. \tag{1}$$

A simpler expression has also been evaluated by Howard *et al.* (Model I), in the form $B=-2\Omega k/\epsilon$.

Another correction introduced by Hellsten[20] for the (k,ω) model[21] corresponds to the curvature correction of Park and Chung.[22] In a (k,ϵ) context, Hellsten's proposal would also involve the $C_{\epsilon 2}$ coefficient, now written in the form

$$C_{\epsilon 2} = C^0_{\epsilon 2}(1 + C_{\mathrm{sc}}B)^{-1},$$

where the Bradshaw–Richardson number was initially defined according to a suggestion of Khodak and Hirsch:[23]

$$B = -|S - 2\Omega|(S - |S - 2\Omega|)k^2/\epsilon^2. \tag{2}$$

However, with this formulation, Hellsten reports an unexpected rise of turbulent kinetic energy in the calculation of the flow in the blade-to-blade channel of a radial compressor. For this reason, his final proposal makes use of the following definition:

$$B = -|S-2\Omega|(S-|S-2\Omega|)/S^2.$$

These models can be used without restriction in the calculation of general flows provided that the definition of the Bradshaw–Richardson number is objective. Introducing the absolute-rotation tensor

$$W_{ij} = \frac{1}{2}\left(\frac{\partial \overline{U_i}}{\partial x_j} - \frac{\partial \overline{U_j}}{\partial x_i}\right) + \varepsilon_{mji}\Omega_m$$

and strain-rate tensor

$$S_{ij} = \frac{1}{2}\left(\frac{\partial \overline{U_i}}{\partial x_j} + \frac{\partial \overline{U_j}}{\partial x_i}\right),$$

objective measures of rotation and strain can be obtained as $\tilde{\Omega}=(W_{ij}W_{ij}/2)^{1/2}$ and $\tilde{S}=(2S_{ij}S_{ij})^{1/2}$, respectively. Definition (2) was initially given by Khodak and Hirsch[23] in the objective form

$$B = -2\tilde{\Omega}(\tilde{S}-2\tilde{\Omega})k^2/\epsilon^2.$$

Following Spalart and Shur,[24] definition (1) can also be made objective as

$$B = -2W_{ik}S_{jk}\left(\frac{k}{\epsilon\tilde{S}}\right)^2\left(\frac{dS_{ij}}{dt} + \Omega_m(\varepsilon_{imn}S_{jn} + \varepsilon_{jmn}S_{in})\right).$$

Note that the last two definitions of the Bradshaw–Richardson number were claimed to unify rotation and curvature effects.

2. Analysis of the model problem

The analysis is performed for the (k,ϵ) turbulence model,[25] but can be extended to any eddy-viscosity model that provides a turbulent time scale. In this context, the Reynolds stresses are modeled as

$$-\overline{u_iu_j} = \nu_t\left(\frac{\partial \overline{U_i}}{\partial x_j} + \frac{\partial \overline{U_j}}{\partial x_i}\right) - \frac{2}{3}k\delta_{ij}, \tag{3}$$

where u_i is the velocity fluctuation along x_i and $\nu_t=C_\mu k^2/\epsilon$ is the eddy viscosity. The HS-Ω flow is governed by the simplified set of model equations,

$$\frac{dk}{dt} = C_\mu\frac{k^2}{\epsilon}S^2 - \epsilon, \tag{4}$$

$$\frac{d\epsilon}{dt} = C_\mu C_{\epsilon1}kS^2 - C_{\epsilon2}\frac{\epsilon^2}{k}. \tag{5}$$

In this situation and at this modeling level, the $C_\mu, C_{\epsilon1}$, and $C_{\epsilon2}$ coefficients can depend—at most—on the values of the nondimensional variable α and parameter β. Equations (4) and (5) can then be combined to give an evolution equation for α in the form

$$\frac{d\alpha}{dt^*} = C_\mu(C_{\epsilon1}-1) - (C_{\epsilon2}-1)\alpha^2 \equiv \Lambda(\alpha), \tag{6}$$

where $t^*=St$. With $\alpha(0)=\alpha_0=\epsilon_0/(Sk_0)$, Eq. (6) constitutes a fully defined dynamical system for the state variable α. Its fixed points α_∞ are the solutions of the equation

$$\Lambda(\alpha_\infty) = 0, \tag{7}$$

and they correspond to the possible equilibrium states of the flow. These states will be realizable if $k\geqslant 0, \epsilon\geqslant 0$, and $|\overline{uv}| \leqslant \sqrt{\overline{u^2}}\sqrt{\overline{v^2}}$ hold when α goes to α_∞. Using relation (3), it is easy to show that the resulting necessary condition for realizability can be written as

$$\alpha_\infty \geqslant 3C_\mu/2. \tag{8}$$

The stability of the fixed point—not to be confused with the stability of the flow—depends on the value of the derivative f' of the function $f(\alpha)=\alpha+\Lambda(\alpha)$ for $\alpha=\alpha_\infty$: if $f'(\alpha_\infty)$ is strictly lower than unity, the fixed point is stable and—in the absence of another stable fixed point—the equilibrium state will attract any initial condition.

In order to discuss the *stability of the flow*, we have to go back to the evolution equations of the turbulent kinetic energy and dissipation rate in the form

$$\frac{1}{k}\frac{dk}{dt^*} = \frac{C_\mu - \alpha^2}{\alpha}, \tag{9}$$

$$\frac{1}{\epsilon}\frac{d\epsilon}{dt^*} = \frac{C_\mu C_{\epsilon1} - C_{\epsilon2}\alpha^2}{\alpha}. \tag{10}$$

We shall consider that the flow is stable (respectively unstable) if the turbulent kinetic energy decreases (respectively increases) with time. For a given, realizable, fixed point α_∞, Eq. (9) shows that the flow in the equilibrium state is neutral if $\alpha_\infty^2=C_\mu$, stable if $\alpha_\infty^2>C_\mu$, and unstable if $\alpha_\infty^2<C_\mu$. Moreover, Eqs. (9) and (10) can be rewritten using relation (7) to give the following relations, holding in the equilibrium state:

$$\left.\frac{1}{k}\frac{dk}{dt^*}\right|_\infty = \left.\frac{1}{\epsilon}\frac{d\epsilon}{dt^*}\right|_\infty = \frac{C_\mu}{\alpha_\infty}\left(\frac{C_{\epsilon2}-C_{\epsilon1}}{C_{\epsilon2}-1}\right)_\infty.$$

These relations have an important consequence for modeling: Considering that C_μ should always remain positive, it appears that the sign of the right-hand side does not depend on the value of C_μ. It is therefore impossible to obtain both stable and unstable flows across the range of β by solely sensitizing this coefficient to the rotation rate.

B. Initially isotropic turbulence

We now consider the unsheared situation. The Reynolds-stress tensor is initially isotropic and if it remains so, rotation does not enter the Reynolds-stress-transport equations. However, early experiments by Wigeland and Nagib[26] did show that the decay rate of turbulence was significantly affected (reduced) by system rotation. Since then, more experiments[27] and numerical simulations[10,11,28,29] have confirmed this reduction in the decay rate. In addition, the data indicate that anisotropy develops—mainly through the length scales: The transverse (normal to the system-rotation vector) scales increase more than the axial scales, while the Reynolds-stress tensor only slightly departs from isotropy. Obviously, these effects are connected with modifications to the energy cascade.[10] The spectral model of Cambon, Bertoglio, and Jeandel,[30] and the analysis of Aupoix, Cousteix, and Liandrat[31] have shown that such modifications could be ex-

TABLE I. Model corrections for the nonlinear effects in rotating homogeneous turbulence. The limit of $C_{\epsilon 2}$ when γ goes to infinity is denoted as $C_{\epsilon 2}^{\infty}$. For the model of Park and Chung, m denotes the exponent of the spectrum at low wave numbers and $C_{\mathrm{nl}}=C_{\epsilon 2}^{0}-1$ by construction.

Reference	$C_{\epsilon 2}$	$C_{\epsilon 2}^{0}$	C_{nl}	$C_{\epsilon 2}^{\infty}$
31	$C_{\epsilon 2}^{0}+C_{\mathrm{nl}}(1+0.1325\gamma)/(1+0.6051\gamma+3.937\gamma^2)$	1.83	0.9	2.73
28	$C_{\epsilon 2}^{0}+C_{\mathrm{nl}}/\gamma$	1.83	0.15	$+\infty$
43	$C_{\epsilon 2}^{0}+C_{\mathrm{nl}}/(1+10\gamma^2)$	1.83	1	2.83
33	$C_{\epsilon 2}^{0}+C_{\mathrm{nl}}/(1+13.04\gamma^2)$	1.71	1.21	2.92
36	$\sqrt{C_{\epsilon 2}^{0\,2}+C_{\mathrm{nl}}/\gamma^2}$	...	...	$+\infty$
37 ($m=2$)	$C_{\epsilon 2}^{0}+C_{\mathrm{nl}}/(1+4.3\gamma^{3/2})$	1.83	0.83	2.67
37 ($m=4$)	$C_{\epsilon 2}^{0}+C_{\mathrm{nl}}/(1+4.3\gamma^{3/2})$	1.7	0.7	2.4
38	$\sqrt{C_{\epsilon 2}^{0\,2}+C_{\mathrm{nl}}/(1+1.525\gamma^2)}$	1.83	3.75	2.67

plained by the explicit action of rotation on the triple correlations (the nonlinear transfer term in Lin's equation). Moreover, a displaced-particle analysis proposed by Jacquin *et al.*[27] introduces the idea of a confinement for the size of the turbulent structures. Such confinement would affect the *transverse* fluctuating motion, and thus explain anisotropy. It would operate at a scale $L_{\Omega}=v'/|\Omega|$ (where v' is the scale of the velocity fluctuations in the transverse plane) and, therefore, leave unaffected the smaller structures. Following this reasoning, one may expect that, at some point, the rotation rate can be high enough for all of the energetic range of the spectrum to be affected, so that the flow would be only marginally modified by any further increase in the rotation rate. We shall refer to this notion as the "strong-rotation limit," above which the effect of rotation on the fluctuating motion saturates. The idea of a transition wave number ($\propto 1/L_{\Omega}$) above which the turbulent structures are not affected by rotation can be found in several model spectra proposed later.[32–35] Accordingly, the rotation-sensitive part of the energetic range should exhibit a slope steeper than the $-5/3$ Kolmogorov slope which is recovered above the transition wave number. In all cases, the upper limit of the rotation-sensitive range is given by a value $k_{\Omega}\propto(\Omega^3/\epsilon)^{1/2}$. Comparison of this value with that of the high end of the energetic range returns the strong-rotation limit.

1. Turbulence-model corrections for the nonlinear effects

Accounting for the nonlinear effects in homogeneous, isotropic turbulence in a rotating frame is rather straightforward: The only term that remains unclosed in the turbulent-kinetic-energy and dissipation-rate equations is the destruction term of the latter. As can be seen in Table I, most of the existing proposals actually rely on the sensitization of the destruction coefficient $C_{\epsilon 2}$ to the ratio $\gamma=(\epsilon/k)/|\Omega|$. The effect of rotation is always to increase the value of $C_{\epsilon 2}$, so that the decay rate of turbulent kinetic energy should be reduced in the HI-Ω situation. However, the different models exhibit two kinds of behavior at high rotation rates: In the models proposed by Bardina *et al.*[28] and Rubinstein and Zhou,[36] the value of $C_{\epsilon 2}$ goes to infinity as the rotation rate increases, whereas it goes to a finite limit ($C_{\epsilon 2}^{\infty}$) with the other models. Aupoix *et al.*[31] were probably the firsts to introduce such a feature in their model, it was supported by the calculation results they obtained using a spectral-closure scheme. Since then, model spectra as those cited in the previous paragraph have further substantiated this point: They allow to deduce consistent expressions of $C_{\epsilon 2}$ as a function of γ (as well as expressions of the eddy-viscosity coefficient C_{μ}). That is the way the models given by Okamoto,[33] Park and Chung,[37] and Thangam, Wang, and Zhou[38] are derived.

Following Bardina *et al.*[28] all the models considered here can be made objective by replacing $|\Omega|$ by $\tilde{\Omega}$.

2. Analysis of the model problem

In the HI-Ω flow, using the (k,ϵ) problem leads to a very simple set of evolution equations:

$$\frac{\partial k}{\partial t}=-\epsilon, \tag{11}$$

$$\frac{\partial \epsilon}{\partial t}=-C_{\epsilon 2}\frac{\epsilon^2}{k}, \tag{12}$$

where the coefficient $C_{\epsilon 2}$ can now depend—at most—on the value of γ. Combining Eqs. (11) and (12) leads to the following dynamical system for the state variable γ:

$$\frac{d\gamma}{dt^{**}}=-(C_{\epsilon 2}-1)\gamma^2\equiv\Pi(\gamma) \tag{13}$$

with $\gamma(0)=\gamma_0=(\epsilon_0/k_0)/|\Omega|$ and $t^{**}=|\Omega|t$. The turbulent-kinetic-energy and dissipation-rate equations can be recast in nondimensional form,

$$\frac{1}{k}\frac{dk}{dt^{**}}=-\gamma, \tag{14}$$

$$\frac{1}{\epsilon}\frac{d\epsilon}{dt^{**}}=-C_{\epsilon 2}\gamma. \tag{15}$$

The fixed points γ_{∞} of the system are given by $\Pi(\gamma_{\infty})=0$. For all the models given in Table I, $C_{\epsilon 2}$ cannot fall to unity and the dynamical system (13) admits only one fixed point: $\gamma_{\infty}=0$. Depending on the model expression of $C_{\epsilon 2}$, one can distinguish several cases. In the first one, we shall consider that $C_{\epsilon 2}^{\infty}$ exists and, therefore, corresponds to the value of $C_{\epsilon 2}$ in the equilibrium state. When this value is inserted in Eqs.

(13)–(15), these can be integrated to give the behavior of the different variables in the equilibrium state (that is, when γ goes to zero and t to infinity):

$$\gamma \propto t^{-1}, \quad k \propto t^{-1/(C_{\epsilon 2}^{\infty}-1)}, \quad \epsilon \propto t^{-C_{\epsilon 2}^{\infty}/(C_{\epsilon 2}^{\infty}-1)}.$$

These are power solutions, the exponents of which do not depend on the value of the rotation rate: They are thus consistent with the idea of a strong-rotation limit. In the second case, we shall consider that $C_{\epsilon 2}^{\infty}$ goes to infinity slower than $1/\gamma^2$ when γ goes to zero. In this case, the fixed point $\gamma_{\infty}=0$ still exists and Eq. (14) shows that the turbulent kinetic energy goes to a constant (not necessarily zero) in the equilibrium state. The evolution of the dissipation rate will depend on the way $C_{\epsilon 2}$ goes to infinity when γ goes to zero. Assuming that it behaves as $1/\gamma$ (this is the case with the models given in Refs. 28 and 36), we find that the dissipation rate experiences an exponential decay given by

$$\epsilon \propto \exp(-A|\Omega|t).$$

The slope of the exponential depends on the rotation rate and the solution is not consistent with the existence of a strong-rotation limit.

A last case of interest, although not applicable to the models given in Table I, is the case where $C_{\epsilon 2}$ can fall to unity. Let us assume that a strictly positive value γ_{∞} exists such that $C_{\epsilon 2}(\gamma_{\infty})=1$. Then γ_{∞} is a fixed point, and integration of Eqs. (14) and (15) in the corresponding equilibrium state yields

$$k \propto \epsilon \propto \exp(-\gamma_{\infty}|\Omega|t).$$

The decreases of both variables are exponential and are enhanced when the rotation rate increases. This is in contradiction with experiment and known physics since, in this case, the decrease of the turbulent kinetic energy should be inhibited.

III. ANALYSIS OF THE CORIOLIS CORRECTION OF HOWARD *et al.*

We shall consider here the proposal of Howard, Patankar and Bordynuik denoted as Model II in Ref. 2 (hereafter called HPB correction). With the notations adopted in Sec. II A 1, the value recommended by Howard *et al.* for C_{sc} is 0.4.

A. Homogeneously sheared turbulence

In the HS-Ω flow, the rotation-dependent expression of $C_{\epsilon 2}$ reads

$$C_{\epsilon 2} = C_{\epsilon 2}^{0}[1 + C_{\mathrm{sc}}\beta(1-2\beta)/\alpha^2]. \tag{16}$$

The fixed points can be obtained using Eq. (7) where the above expression of $C_{\epsilon 2}$ has been inserted, that is,

$$\alpha_{\infty}^2 = \frac{-C_{\epsilon 2}^{0}C_{\mathrm{sc}}\beta(1-2\beta) + C_{\mu}(C_{\epsilon 1}-1)}{C_{\epsilon 2}^{0}-1}. \tag{17}$$

We see that α_{∞} may not exist and that, otherwise, its value will depend on the rotation rate through the value of β. Introducing

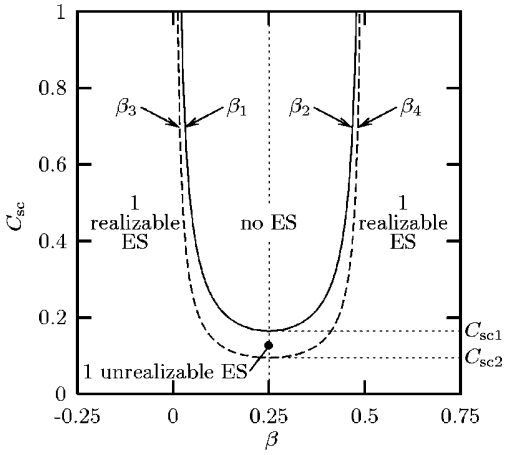

FIG. 1. Existence and realizability of the equilibrium states (ES) predicted with the HPB-corrected (k,ϵ) model in homogeneously sheared turbulence as a function of C_{sc}.

$$C_{\mathrm{sc1}} = \frac{8C_{\mu}}{C_{\epsilon 2}^{0}}(C_{\epsilon 1}-1),$$

it is a simple matter to conclude that a single positive α_{∞} exists (i) for all β, when $C_{\mathrm{sc}} \leqslant C_{\mathrm{sc1}}$; (ii) if and only if $\beta \in]-\infty,\beta_1] \cup [\beta_2,+\infty[$, when $C_{\mathrm{sc}} > C_{\mathrm{sc1}}$, with

$$\beta_{\frac{1}{2}} = \frac{1}{4} \mp \frac{1}{4}\sqrt{1 - \frac{8C_{\mu}}{C_{\mathrm{sc}}C_{\epsilon 2}^{0}}(C_{\epsilon 1}-1)}.$$

In order to investigate the realizability of the equilibrium states when they exist, Eq. (17) can be inserted in condition (8) to give

$$2\beta^2 - \beta + \frac{C_{\mu}}{C_{\mathrm{sc}}C_{\epsilon 2}^{0}}\left[C_{\epsilon 1} - 1 - \frac{9}{4}C_{\mu}(C_{\epsilon 2}^{0}-1)\right] \geqslant 0.$$

Introducing now

$$C_{\mathrm{sc2}} = \frac{8C_{\mu}}{C_{\epsilon 2}^{0}}\left[C_{\epsilon 1} - 1 - \frac{9}{4}C_{\mu}(C_{\epsilon 2}^{0}-1)\right],$$

we find that there exists one single *realizable* equilibrium state (i) for all β, when $C_{\mathrm{sc}} \leqslant C_{\mathrm{sc2}}$; (ii) if and only if $\beta \in]-\infty,\beta_3] \cup [\beta_4,+\infty[$, when $C_{\mathrm{sc}} > C_{\mathrm{sc2}}$, with

$$\beta_{\frac{3}{4}} = \frac{1}{4} \mp \frac{1}{4}\sqrt{1 - \frac{8C_{\mu}}{C_{\mathrm{sc}}C_{\epsilon 2}^{0}}\left[C_{\epsilon 1} - 1 - \frac{9}{4}C_{\mu}(C_{\epsilon 2}^{0}-1)\right]}.$$

It can be easily checked that the fixed point is stable when it exists. The values of β_1 to β_4 have been plotted as functions of C_{sc} in Fig. 1. We can see that the recommended value $C_{\mathrm{sc}}=0.4$ leads to the most general case: ranges of β with no fixed point, one unrealizable fixed point, or one realizable fixed point.

When the fixed point exists, the results obtained in Sec. II show that the stability of the flow can be discussed by comparing the values of α_{∞} and $C_{\mu}^{1/2}$. This leads to introducing two other particular values of β,

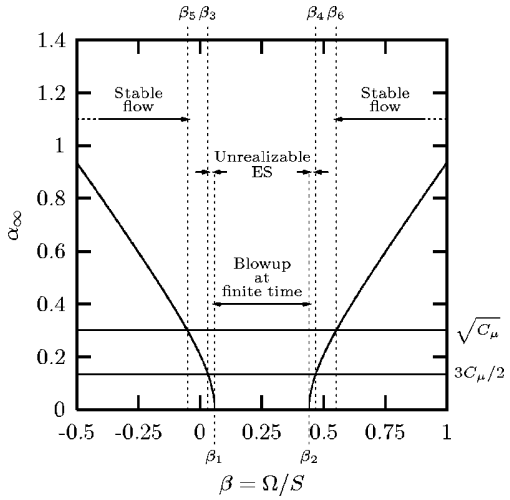

FIG. 2. Fixed-point diagram obtained with the HPB-corrected (k,ϵ) model in homogeneously sheared turbulence. The fixed point α_∞ is plotted as a function of β. Unstable flow is obtained when the curve is below $C_\mu^{1/2}$. If it goes below $3C_\mu/2$, the equilibrium state is unrealizable.

$$\beta_{\frac{5}{6}} = \frac{1}{4} \mp \frac{1}{4}\sqrt{1 + 8C_\mu \frac{C^0_{\epsilon 2} - C_{\epsilon 1}}{C_{\rm sc} C^0_{\epsilon 2}}},$$

and to conclude that, in the equilibrium state, the flow will be (a) neutrally stable if $\beta=\beta_5$ or $\beta=\beta_6$, (b) stable if $\beta \in]-\infty,\beta_5[\cup]\beta_6,+\infty[$, (c) unstable if $\beta \in]\beta_5,\beta_1] \cup [\beta_2,\beta_6[$.

In the absence of fixed point (that is, if $\beta \in]\beta_1,\beta_2[$), there is no simple way to evaluate the stability of the flow. However, for this particular correction method, we have been able to obtain closed-form solutions to the evolution problem for any value of β. These are given in Appendix A, and show that the system can experience a *blowup at finite time*: in the range $\beta \in]\beta_1,\beta_2[$, k and ϵ go to infinity while α goes to zero at the nondimensional time t_1^* given by

$$t_1^* = (ab)^{-1/2} \arctan\sqrt{\alpha_0^2 a/b},$$

with

$$a = C^0_{\epsilon 2} - 1, \quad b = C_{\rm sc} C^0_{\epsilon 2}\beta(1-2\beta) - C_\mu(C_{\epsilon 1} - 1).$$

The flow could therefore be termed unstable in this case, but such solutions are grossly unphysical.

The fixed-point diagram is given in Fig. 2 for $C_{\rm sc}=0.4$. The equilibrium value α_∞ is plotted as a function of β, the location of the corresponding curve relative to $C_\mu^{1/2}$ and $3C_\mu/2$ allows graphical determination of the ranges of β where the flow is stable ($\alpha_\infty > C_\mu^{1/2}$) and realizable ($\alpha_\infty > 3C_\mu/2$) in the equilibrium state.

B. Initially isotropic turbulence

In the HI-Ω flow, $C_{\epsilon 2}$ becomes rotation dependent through the state variable γ,

$$C_{\epsilon 2} = C^0_{\epsilon 2}(1 - 2C_{\rm sc}/\gamma^2),$$

and the dynamical system takes the form

$$\frac{d\gamma}{dt^{**}} = 2C_{\rm sc}C^0_{\epsilon 2} - (C^0_{\epsilon 2} - 1)\gamma^2 \quad \text{with } \gamma(0) = \gamma_0. \tag{18}$$

It admits one realizable equilibrium state for which $\gamma_\infty^2 = 2C_{\rm sc}C^0_{\epsilon 2}/(C^0_{\epsilon 2} - 1)$, that is, $\gamma_\infty = 1.29$ with $C_{\rm sc}=0.4$ and $C^0_{\epsilon 2} = 1.92$. According to the results obtained in Sec. II B 2, the fixed point corresponds to the case where $C_{\epsilon 2}$ falls to unity, and each of the closure variables experiences an exponential decrease in the asymptotic regime.

Consistency of these results with the HS-Ω analysis when $|\beta|$ goes to infinity is easily checked, since in this case

$$\alpha_\infty \to \sqrt{\frac{2C_{\rm sc}C^0_{\epsilon 2}}{C^0_{\epsilon 2} - 1}\beta^2}, \quad \gamma = \frac{\alpha}{|\beta|} \to \sqrt{\frac{2C_{\rm sc}C^0_{\epsilon 2}}{C^0_{\epsilon 2} - 1}} = \gamma_\infty.$$

C. Discussion

The above results show that the HPB correction method is rather efficient in mimicking the effects of the shear/Coriolis instability: The unstable-flow range between β_5 and β_6 extends slightly and symmetrically outside the 0–0.5 range given by linear-stability analysis (see Table II). As mentioned above, the lower bound should be negative so that the value -0.05 obtained for β_5 cannot be criticized. We may, however, have some restriction on the upper bound ($\beta_6 \approx 0.55$), since it is highly probable that the flow should return stable for $\beta=0.5$. We found that this point has a direct consequence on the prediction of the velocity profile in the neutral-stability region of the channel flow with spanwise rotation. As a matter of fact, if we consider that viscous effects and turbulent diffusion can be neglected in this region, the closure equations can be written as

$$0 = C_\mu \frac{k^2}{\epsilon}\frac{\partial \overline{U}}{\partial y} - \epsilon, \quad 0 = C_{\epsilon 1}C_\mu k \frac{\partial \overline{U}}{\partial y} - C_{\epsilon 2}\frac{\epsilon^2}{k}.$$

These equations are identical to those obtained at the neutral-flow fixed points in the HS-Ω flow, and can therefore only be satisfied if

$$\Omega(\partial \overline{U}/\partial y)^{-1} = \beta_5 \text{ or } \beta_6.$$

The value of β_5 is negative and would correspond to negative velocity gradients close to the suction side of the chan-

TABLE II. Remarkable points of the fixed-point diagram obtained with the HPB-corrected (k,ϵ) model and some particular values of $C_{\rm sc}$ in homogeneously sheared turbulence.

$C_{\rm sc}$	β_1	β_2	β_3	β_4	β_5	β_6
0.4	0.058	0.442	0.032	0.468	−0.051	0.551
$C_{\rm sc1}=0.165$	0.25	0.25	0.124	0.376	−0.112	0.612
$C_{\rm sc2}=0.0951$	⋯	⋯	0.25	0.25	−0.175	0.675

nel. The reasoning fails in this region where the flow is not fully turbulent. We can therefore conclude that the predicted slope of the velocity profile should be equal to $\Omega/\beta_6 \approx 1.8\Omega$ across the neutral-stability region, and that the latter corresponds to the region where diffusion can be neglected. A similar reasoning can be made with the exact, unclosed, statistical equations, and may explain why the neutral-stability region does not reduce to a single point in the real flow too (the question was raised by Johnston *et al.* in Ref. 12). From experiment and simulation, we expect that the slope should be fairly close to 2Ω, so that the result obtained with the HPB correction is acceptable although slightly underestimated.

The blowups at finite time encountered in the range β_1–β_2 are much more a matter of concern. They are reminiscent of the diverging solutions obtained by Ji and Durbin[39] in the absence of a stable equilibrium state too, but in a slightly different context: second-order closure and turbulence subject to rotation and stable stratification. Also, we believe that this property of the dynamical system is connected with the unexpected rise of turbulent kinetic energy reported by Hellsten[20] in the computation of the flow in a centrifugal-compressor rotor. As a matter of fact, the fixed-point diagram given in Appendix B confirms that the initial form of Hellsten's correction (see Sec. II A 1) leads to roughly the same kind of behavior as the HPB correction. As the latter is concerned, a possible remedy consists in lowering the value of C_{sc} below C_{sc1}, so as to obtain a stable equilibrium state for any value of Ω/S. This is apparent in Table II, where the particular values of β arising from the analysis are given for $C_{sc}=C_{sc1}$ and $C_{sc}=C_{sc2}$: when C_{sc} goes below C_{sc1}, the range β_1–β_2 is removed from the fixed-point diagram. Unfortunately, the values reached by β_6 indicate that such a recalibration may have a detrimental effect on the predicted slope of the velocity profile in the neutral-stability region of the channel flow. In order to check this point and validate the connection made above between the value of β_6 and the slope of the velocity profile, calculations of the channel flow have been performed with the values of C_{sc} given in Table II. The flow has been computed with $\mathrm{Ro}_m=U_m/(2\Omega h)=2$ and $\mathrm{Re}_m=2U_m h/\nu=5800$, where h is half the distance between the walls and U_m the bulk velocity. The predicted profiles of the local mean-velocity gradient across the channel are plotted in Fig. 3, together with constant values estimated as Ω/β_6. The simulation results of Kristoffersen and Andersson[4] at these Reynolds and Rossby numbers are also plotted for reference. It can be seen that all profiles do exhibit the constant plateau corresponding to the neutral-stability region. The level of this plateau (equal to unity, if the slope were equal to 2Ω) decreases with the value of C_{sc}, in a remarkable agreement with the theoretical estimates. When $C_{sc}=C_{sc2}$, the predicted slope underestimates the simulation data by more than 20%.

The behavior of the model at high-rotation rates is also questionable: With or without mean shear, increasing rotation can never bring the value of γ below 1.29 in the asymptotic regime, a value which is much higher than those recorded in available experiments. (For instance, the data of Jacquin *et al.*[27] at their highest rotation rate give values of γ about 0.2 still steadily decreasing at the last measurement station). Moreover, in this high-rotation regime ($\gamma=1.29$), the time decrease of the closure variables remains dependent on the rotation rate, and further increase in the rotation rate results in a faster decrease of the turbulent kinetic energy. The model is therefore not consistent with a strong-rotation limit and disagrees with experiment. The dynamical-system analysis of the HI-Ω flow shows that all these deficiencies are connected with the possibility for the coefficient $C_{\epsilon 2}$ to fall to unity.

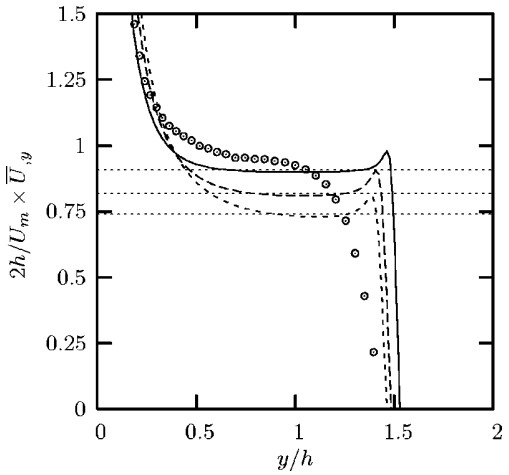

FIG. 3. Profiles of the local mean-velocity gradient obtained with the HPB-corrected (k,ϵ) model and some particular values of C_{sc} in the plane-channel flow with spanwise rotation. The pressure side is located at $y/h=0$ and the suction side at $y/h=2$. (—), $C_{sc}=0.4$; (– –), $C_{sc}=C_{sc1}$; (- - -), $C_{sc}=C_{sc2}$; dotted lines, theoretical estimates of the predicted slopes $(\mathrm{Ro}_m^{-1}\beta_6^{-1})$; symbols, DNS results of Kristoffersen and Andersson (Ref. 4).

IV. THE NEW CORIOLIS CORRECTION

In this section we shall work on the HPB correction with the aim of suppressing the blowups at finite time, and restoring a physically consistent behavior at high-rotation rates. To this end, we shall first design the correction method in the framework of homogeneous turbulence, with the basic requirements that (i) it produces a single, stable, and realizable fixed point for any value of β in the HS-Ω flow, (ii) it reduces to a proven model for the nonlinear effects in the HI-Ω flow.

In a second step, we shall generalize the resulting formulation so that the final model can be used without any ambiguity in nonhomogeneous flows.

A. Design of the correction method

With the simplifications and notations used in the HS-Ω flow, one way to begin the design of the model is to write the expression of $C_{\epsilon 2}$ in the form

$$C_{\epsilon 2} = C_{\epsilon 2}^0\left[1 + F_{\mathrm{nl}}(\beta,\alpha) + F_{\mathrm{sc}}(\theta,\alpha)\right], \tag{19}$$

where

$$\theta = \frac{\Omega(S-2\Omega)}{S\times\epsilon/k} = \beta(1-2\beta)/\alpha$$

is a *mixed* Bradshaw–Richardson number (normalization involves both the mean-flow and turbulent time scales).

The F_{nl} function is the correction for nonlinear effects, any model given in Sec. II B 1 can be used here. Our preference goes to the model of Park and Chung[37] which is based on a model spectrum with a −2 slope in the wave-number range affected by rotation, and leads to a bounded evolution of $C_{\epsilon 2}$ consistent with the idea of a strong-rotation limit. Making this model objective by the use of $\tilde{\Omega}$, we write

$$F_{\mathrm{nl}} = \frac{(C^0_{\epsilon 2} - 1)/C^0_{\epsilon 2}}{1 + a\left(\dfrac{\alpha}{|1/2 - \beta|}\right)^{3/2}}. \tag{20}$$

The F_{sc} function is the correction for the shear Coriolis instability. It will be defined subject to several conditions that must guarantee a correct mathematical behavior (realizability, existence of a stable equilibrium state for any value of β), as well as render a physically consistent phenomenology (flow-stability characteristics in the equilibrium state). We have retained the following.

(a) The correction is inactive in the limit of vanishing shear rates, i.e.,

$F_{\mathrm{sc}} \to 0$ when $\alpha \to \infty$.

(b) It is roughly equivalent to the HPB correction in the vicinity of the neutral-flow fixed points, i.e.,

$F_{\mathrm{sc}}(\theta, \alpha) \approx K\theta/\alpha$ when $\theta \to 0$,

K being a constant equivalent to the C_{sc} constant of the HPB correction.

(c) The equilibrium state is always realizable, i.e.,

for all β, $\alpha_\infty \geqslant 3C_\mu/2$.

(d) The flow remains stable in the limit of high rotation-to-shear ratio, i.e.,

$\alpha_\infty \geqslant \sqrt{C_\mu}$ when $|\beta| \to \infty$.

These conditions can be satisfied by taking F_{sc} in the form

$$F_{\mathrm{sc}}(\theta, \alpha) = \frac{C_{\mathrm{sc}}}{\alpha}[\tanh(b\theta + c) - d]. \tag{21}$$

Condition (a) is automatically satisfied. Linearizing F_{sc} around $\theta = 0$ then gives

$$F_{\mathrm{sc}} \sim \frac{C_{\mathrm{sc}}}{\alpha}[\tanh c - d + b(1 - \tanh^2 c)\theta],$$

so that, if $\tanh c \approx d$, condition (b) will be satisfied with

$$K = C_{\mathrm{sc}} b(1 - \tanh^2 c). \tag{22}$$

In order to check that condition (c) can be satisfied, we rewrite Eq. (7) taking into account the definition (19) of $C_{\epsilon 2}$ and obtain

$$(C^0_{\epsilon 2} - 1)\frac{2 + A}{1 + A}\alpha_\infty^2 + C^0_{\epsilon 2} C_{\mathrm{sc}} B \alpha_\infty - C_\mu(C_{\epsilon 1} - 1) = 0, \tag{23}$$

where

$$A = \left|\frac{\alpha_\infty}{1/2 - \beta}\right|^{3/2}, \quad B = \tanh(b\theta_\infty + c) - d.$$

Equation (23) can be considered as a quadratic equation for α_∞ with a single positive root. It is therefore strictly equivalent to

$$\alpha_\infty = \frac{1 + A}{2 + A} \times \frac{-C^0_{\epsilon 2} C_{\mathrm{sc}} B + \sqrt{\Delta}}{2\left(C^0_{\epsilon 2} - 1\right)}, \tag{24}$$

with

$$\Delta = C^{0\,2}_{\epsilon 2} C^2_{\mathrm{sc}} B^2 + 4C_\mu(C_{\epsilon 1} - 1)(C^0_{\epsilon 2} - 1)\frac{2 + A}{1 + A}.$$

It can be shown that the right-hand side of Eq. (24) is an increasing function of A and a decreasing function of B. Whatever the values of α_∞ and β are, A is positive and B is in the range $]-1-d, 1-d[$. A lower bound for the value of the fixed point α_∞ can therefore be obtained taking $A = 0$ and $B = 1 - d$ in Eq. (24); it reads

$$\alpha_\infty \geqslant \frac{-C^0_{\epsilon 2} C_{\mathrm{sc}}(1 - d)}{4(C^0_{\epsilon 2} - 1)} + \frac{\sqrt{C^{0\,2}_{\epsilon 2} C^2_{\mathrm{sc}}(1 - d)^2 + 8C_\mu(C_{\epsilon 1} - 1)(C^0_{\epsilon 2} - 1)}}{4(C^0_{\epsilon 2} - 1)}.$$

Specifying that this lower bound is equal to $3C_\mu/2$, we find a sufficient condition on d for condition (c) to be satisfied:

$$d = 1 - \frac{1}{C_{\mathrm{sc}} C^0_{\epsilon 2}}\left[\frac{2}{3}(C_{\epsilon 1} - 1) - 3C_\mu(C^0_{\epsilon 2} - 1)\right]. \tag{25}$$

Turning now to condition (d), we note that Eq. (24) can also be used to place a finite upper bound on α_∞. It follows that, if the fixed point exists, α_∞ remains finite when $|\beta|$ goes to infinity. This result can then be used together with Eqs. (19)–(21) to state that $C_{\epsilon 2}$ takes a constant value, equal to $2C^0_{\epsilon 2} - 1 - C^0_{\epsilon 2} C_{\mathrm{sc}}(1 + d)/\alpha_\infty$, in the equilibrium states obtained when $|\beta|$ goes to infinity. When this value is inserted in Eq. (7), we get a quadratic equation with only one positive root a_∞ (the limit of α_∞ when $|\beta|$ goes to infinity) given by

$$a_\infty = \frac{C^0_{\epsilon 2} C_{\mathrm{sc}}(1 + d)}{4(C^0_{\epsilon 2} - 1)} + \frac{\sqrt{C^{0\,2}_{\epsilon 2} C^2_{\mathrm{sc}}(1 + d)^2 + 8C_\mu(C_{\epsilon 1} - 1)(C^0_{\epsilon 2} - 1)}}{4(C^0_{\epsilon 2} - 1)}.$$

In practice, the value of C_{sc} will be drawn from this equation after having specified a value of a_∞ [higher than $C_\mu^{1/2}$ in agreement with condition (d)]. Eliminating d with Eq. (25), we get

$$C_{\mathrm{sc}} = \frac{[3a_\infty(C^0_{\epsilon 2} - 1) + C_{\epsilon 1} - 1](2a_\infty - 3C_\mu)}{6a_\infty C^0_{\epsilon 2}}. \tag{26}$$

At this stage, we note that the expression of $C_{\epsilon 2}$ is dependent on the shear rate *in the absence of rotation.* This dependency takes the form

$$C_{\epsilon 2} = C^0_{\epsilon 2} + \frac{C^0_{\epsilon 2} - 1}{1 + a(2\alpha)^{3/2}} + \frac{C_{\rm sc} C^0_{\epsilon 2}}{\alpha}(\tanh c - d),$$

and should not affect the generality of the model if the value of $C_{\epsilon 2}$ is adequate in the usual calibration case: the logarithmic layer of wall-bounded flows. With the (k,ϵ) model, the behavior of the main variables is known there, given by

$$\epsilon = \frac{u_\tau^3}{\kappa y}, \quad k = \frac{u_\tau^2}{\sqrt{C_\mu}}, \quad \frac{\partial \overline{U}}{\partial y} = \frac{u_\tau}{\kappa y},$$

where u_τ is the friction velocity and κ the Kármán constant. According to our expression of $C_{\epsilon 2}$, this coefficient would take the following value in the logarithmic layer:

$$C^\kappa_{\epsilon 2} = C^0_{\epsilon 2} + \frac{C^0_{\epsilon 2} - 1}{1 + a(2\sqrt{C_\mu})^{3/2}} + \frac{C_{\rm sc} C^0_{\epsilon 2}}{\sqrt{C_\mu}}(\tanh c - d).$$

The standard value $C^\kappa_{\epsilon 2} = 1.92$ can thus be recovered by taking

$$\tanh c = d - \left(C^0_{\epsilon 2} - C^\kappa_{\epsilon 2} + \frac{C^0_{\epsilon 2} - 1}{1 + a(2\sqrt{C_\mu})^{3/2}} \right) \frac{\sqrt{C_\mu}}{C_{\rm sc} C^0_{\epsilon 2}}. \quad (27)$$

B. Generalization and final calibration of model constants

Generalization will be performed by defining objective Rossby and Bradshaw–Richardson numbers that should reduce to γ and θ in the HI-Ω and HS-Ω flows, respectively. We retain

$$\widetilde{\rm Ro} = \frac{\epsilon}{\tilde{\Omega} k}$$

and

$$\widetilde{\rm BR} = -\frac{2k}{\tilde{S}^3 \epsilon} W_{ik} S_{jk} \left(\frac{dS_{ij}}{dt} + \Omega_m (\varepsilon_{imn} S_{jn} + \varepsilon_{jmn} S_{in}) \right).$$

The definition of $\widetilde{\rm Ro}$ directly follows from the suggestion of Bardina *et al.*,[28] while the definition of $\widetilde{\rm BR}$ is adapted from the proposal of Spalart and Shur.[24] The model expression for $C_{\epsilon 2}$ can now be written as

$$C_{\epsilon 2} = C^0_{\epsilon 2} + \frac{C^0_{\epsilon 2} - 1}{1 + a\,\widetilde{\rm Ro}^{3/2}} + C^0_{\epsilon 2} C_{\rm sc} \frac{\tilde{S} k}{\epsilon} [\tanh(b\widetilde{\rm BR} + c) - d]. \quad (28)$$

Calibration of the constants involves two sets of standard values: those given by Launder and Sharma[40] for the (k,ϵ) model and those recommended by Park and Chung[37] for their Coriolis correction, that is,

$$C_\mu = 0.09, \quad C_{\epsilon 1} = 1.44, \quad C^\kappa_{\epsilon 2} = 1.92$$

and

$$C^0_{\epsilon 2} = 1.83, \quad a = 4.3.$$

At this stage, a value of K about 0.4 and a value of a_∞ higher than $C_\mu^{1/2}$ have to be selected. We choose

TABLE III. Calculation of the modeling constants for the present model. Given the initial choice $a_\infty = 0.3$ and $K = 0.5$, calculation of the coefficients proceeds from left to right.

Constant	$C_{\rm sc}$	d	c	b
Determining equation	(26)	(25)	(27)	(22)
Value	0.119	0.682	0.453	5.13

$$K = 0.5, \quad a_\infty = \sqrt{C_\mu} = 0.3.$$

The remaining constants are determined using the relations established in the preceding section, Table III gives the determining equation and the final value obtained for each of them.

Figures 4 and 5 show the fixed-point diagram obtained with the present model and illustrate the influence of the constants a_∞ and K on this diagram. All plots are obtained by numerically solving Eq. (7); they exhibit the desired properties: a single, stable, and realizable fixed point exists for any value of β, the lower bound of the unstable-flow range is slightly below $\beta = 0$, and the upper bound is close to $\beta = 0.5$. With $K = 0.5$ and $a_\infty = 0.3$, we find that the unstable-flow range goes from $\beta \approx -0.039$ to 0.518. The figures show that the effect of each constant is rather distinct: The influence of a_∞ is limited to the stable-flow range and that of K to the transition between stable and unstable flows. Calibration of the model in the stable-flow range is not easy due to the lack of physical data, the value $a_\infty = 0.3$ selected here is in agreement with the RDT results of Bertoglio[17] (see following section). As the transition range is concerned, Fig. 5 shows that the sensitivity to the value of K is not high, the choice $K = 0.5$ has been made primarily for simplicity. However, the channel flow with spanwise rotation presents such a transition. Calculations presented in the following section do not contradict this choice.

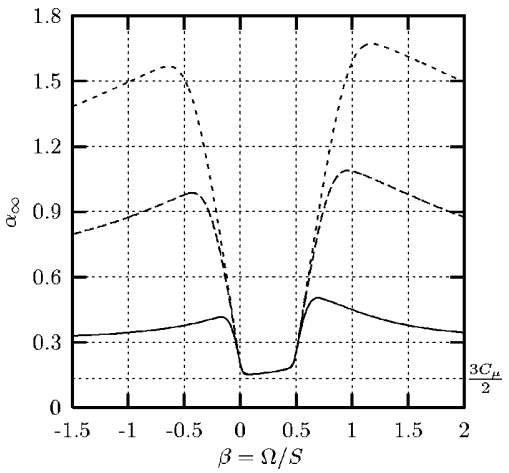

FIG. 4. Influence of the value of a_∞ on the fixed-point diagram obtained with the present model in homogeneously sheared turbulence. All calculations are performed with $K = 0.5$. (—), $a_\infty = C_\mu^{1/2}$; (– –), $a_\infty = 2C_\mu^{1/2}$; (- - -), $a_\infty = 3C_\mu^{1/2}$.

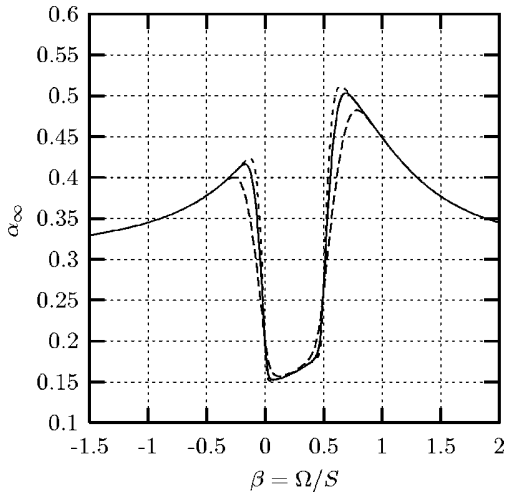

FIG. 5. Influence of the value of K on the fixed-point diagram obtained with the present model in homogeneously sheared turbulence. All calculations are performed with $a_\infty = C_\mu^{1/2}$. (– –), $K=0.25$; (—), $K=0.5$; (- - -), $K=0.75$.

C. Validation

In the situation of initially isotropic turbulence in a rotating frame, the present model becomes strictly equivalent to the model of Park and Chung.[37] In Ref. 37, the authors show that the model is in excellent agreement with the experimental results of Wigeland and Nagib[26] when a value of 1.83 is selected for $C_{\epsilon 2}^0$. A similar agreement with the experiments of Jacquin *et al.*,[27] and direct numerical simulations by Mansour, Cambon, and Speziale (see Ref. 37) is also claimed when the value of $C_{\epsilon 2}^0$ is adjusted so as to account for the initial spectra of the experimental data.

When shear is present, the LES results of Bardina *et al.*[11] can be used to assess the performance of the model in the unstable-flow range. Figure 6 shows the results of calculations performed for the three cases documented by Bardina *et al.* ($\beta=0$, 0.25, and 0.5) together with results obtained using the HPB-corrected (k,ϵ) model. When $\beta=0$, the latter model reduces to the standard model and gives the same evolutions of turbulent kinetic energy and dissipation rate. The present model remains very close to the standard model with $\alpha_\infty \approx 0.205$ (instead of 0.202) and $C_{\epsilon 2} \approx 1.95$ (instead of 1.92). As a result, the evolution of the closure variables is virtually identical for the two models. When $\beta=0.25$, the figure illustrates the blowup at finite time experienced with the HPB-corrected (k,ϵ) model, while the present model shows a physically consistent behavior: the growth rates of the closure variables remain finite, although slightly lower than those obtained in LES. In the last case ($\beta=0.5$), the flow should be close to neutral; the present model again shows a sensible improvement over the HPB-corrected (k,ϵ) model, even if the predicted flow remains slightly unstable. Comparison with the RDT results of Bertoglio[17] in Fig. 7 unables one to assess the behavior of the model in the stable range. Time evolution of the turbulent kinetic energy is plotted for $\beta=0$ and -0.25; the figure shows that the rates of

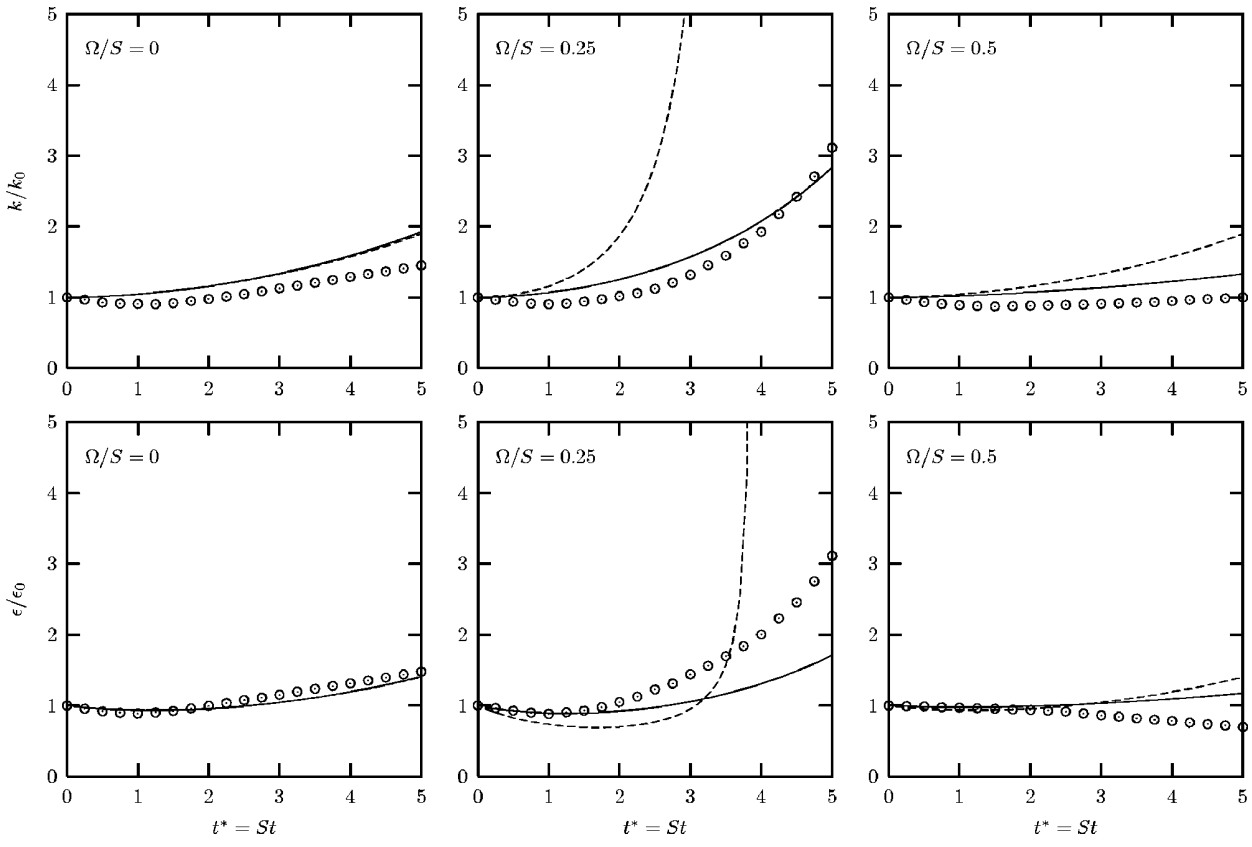

FIG. 6. Time evolutions of the turbulent kinetic energy and dissipation rate for homogeneously sheared turbulence in a rotating frame. ⊙: LES results of Bardina, Ferziger, and Reynolds (Ref. 11). Model calculations are performed with $\alpha_0=0.296$. (–), Present model; (– –), HPB-corrected (k,ϵ) model.

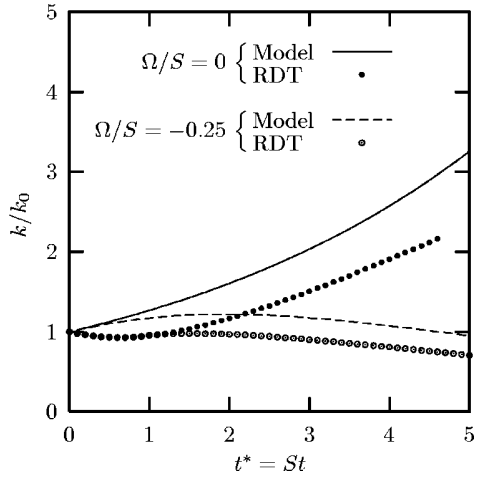

FIG. 7. Time evolution of the turbulent kinetic energy for homogeneously sheared turbulence in a rotating frame. Comparison between the results obtained with the present model and the RDT results of Bertoglio (Ref. 17). Model calculations are performed with $\alpha_0 = 0.204$.

increase/decrease are in good agreement as soon as the memory of the initial condition is lost. Attention is brought to the fact that trying to catch the evolution of the flows simulated by Bertoglio[17] and Bardina *et al.*[11] at early times with an eddy-viscosity model like ours is illusive: This kind of model instantaneously correlates the velocity fluctuations when mean shear is present, while LES as well as RDT take some time to buildup significant shear stress, and hence turbulence production.

As already mentioned, the plane-channel flow with spanwise rotation is an important test case for practical applications. The DNS results of Kristoffersen and Andersson,[4] and Lamballais, Lesieur, and Métais[5] have been used here to validate the model. We shall denote as u_τ the quadratic mean of the friction velocities on the pressure wall ($u_{\tau p}$) and suction wall ($u_{\tau s}$), and introduce the corresponding Reynolds number: $\mathrm{Re}_\tau = u_\tau h/\nu$. Model calculations have been performed with the HPB-corrected (k,ϵ) model and the present model so as to match the mean Reynolds and Rossby numbers obtained in the simulations: $\mathrm{Re}_m = 5800$ and $\mathrm{Ro}_m = 2$ for the data of Kristoffersen and Andersson, $\mathrm{Re}_m = 5000$ and $\mathrm{Ro}_m = 2/3$ for the data of Lamballais *et al.* Both models are used with the low-Reynolds-number treatment of Launder and Sharma.[40] Figure 8 shows the mean-velocity profiles obtained in these flows, and it can be seen that the two models perform well in this situation. We note that the slope of the profile in the neutral-stability region is slightly better predicted with the present model. This is consistent with our theoretical estimates according to which the slope should be equal to $\Omega/0.518 = 1.93\Omega$ instead of $\Omega/0.551 = 1.81\Omega$ with the HPB correction. Location of the mean-velocity maximum is also better predicted with the present model; this is striking at the highest rotation rate. As the friction coefficients are concerned, Tables IV and V indicate that the HPB correction is more accurate at these low Reynolds numbers. However the Launder–Sharma low-Reynolds-number treatment is known to underestimate the friction coefficient at low bulk Reynolds numbers, and our results are more in line with those obtained in the absence of rotation. The good result obtained for the friction coefficient with the HPB correction could therefore be a case of compensating errors.

TABLE IV. Channel flow with spanwise rotation at $\mathrm{Re}_m = 5800$ and $\mathrm{Ro}_m = 2$. Model calculations compared with the DNS data of Kristoffersen and Andersson (Ref. 4). The friction coefficient is defined as $C_{fm} = 2u_\tau^2/U_m^2$.

	Re_τ	C_{fm}	$u_{\tau p}/u_\tau$
DNS	194	0.008 60	1.207
HPB correction	190	0.008 59	1.24
Present model	172.4	0.007 07	1.22

V. CONCLUSION

We have presented the development and validation of a linear (k,ϵ) model modified so as to account for the main influences of system rotation on turbulence: the inhibition of the cascade to small scales and the shear/Coriolis instability.

The development of the model is based on our suggestion that physical consistency of the turbulence model should be examined with reference to the equilibrium states obtained in time-evolving homogeneous turbulence (with and without homogeneous shear). This is a distinction with ear-

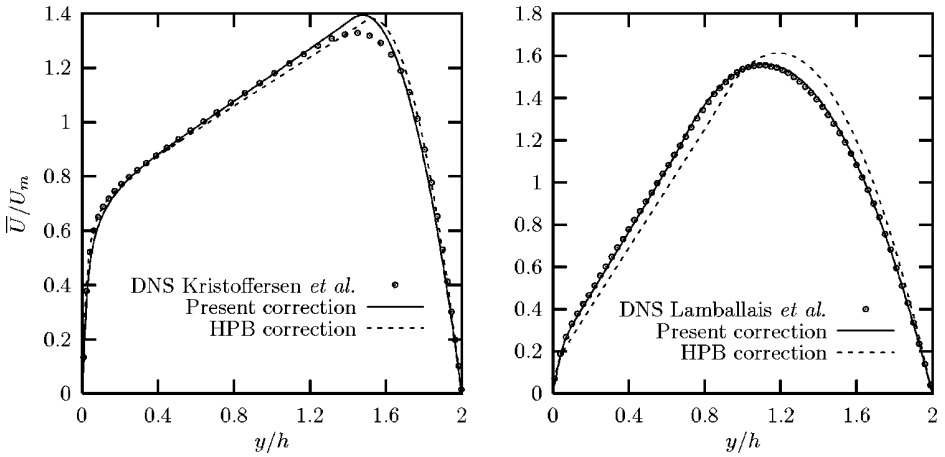

FIG. 8. Mean-velocity profiles obtained in the channel flow with spanwise rotation. Comparison between the DNS results obtained by Kristoffersen and Andersson (Ref. 4) and Lamballais, Lesieur, and Métais (Ref. 5) with model calculations performed using the present model and the HPB-corrected (k,ϵ) model.

TABLE V. Channel flow with spanwise rotation at $\mathrm{Re}_m=5000$ and $\mathrm{Ro}_m=2/3$. Model calculations compared with the DNS data of Lamballais, Lesieur, and Métais (Ref. 5).

	Re_τ	C_{fm}	$u_{\tau p}/u_\tau$
DNS	113	0.004 09	1.15
HPB correction	110.8	0.003 93	1.13
Present model	99.6	0.003 17	1.07

lier proposal[41] and practices. Our motivation is that a first guess on the effect of a model constant can be misleading: For instance, the fact that the HPB correction leads to the decrease of the destruction coefficient $C_{\epsilon 2}$ when rotation is increased led Speziale *et al.*[41] to reject such modifications on the ground that the predicted dissipation rate should increase with rotation. However, the dynamical-system analysis of the unsheared flow indicates without any doubt that this is not the case in the equilibrium state, where it is the evolution of the turbulent kinetic energy which is questionable.

Another issue is the treatment of the eddy viscosity and its coefficient C_μ. From a phenomenological point of view, sensitizing C_μ to the rotation rate would be natural: Model spectra like those cited in Sec. II B lead to rotation-sensitive expressions of the eddy-viscosity coefficient in unsheared turbulence.[34,34] Also, the basic mechanism responsible for the shear/Coriolis instability affects the Reynolds shear stress, and would therefore probably need another correction to C_μ. However, we consider that the eddy viscosity is undefined in unsheared turbulence ($\nu_t=-\overline{uv}[\partial\overline{U}/\partial y]^{-1}$), and that the dynamical-system analysis of the sheared flow shows unambiguously that a modification to the eddy-viscosity coefficient alone is not able to bring the prediction from unstable flow to stable flow when the rotation-to-shear ratio varies. This points out that our modification to $C_{\epsilon 2}$ for the shear/Coriolis cannot be considered as phenomenological. Instead, our approach is based on the idea that physically consistent predictions can be obtained in target configurations if some mathematical properties are satisfied.

We believe that the present model should prove useful in practical computation of turbulent flows in rotating frames: Its results are physically consistent with the known effects of the Coriolis acceleration on turbulence, and it should be free from the problem of blowup at finite time. The definition of the Bradshaw–Richardson number used here as a sensor of the rotation-to-shear ratio was initially proposed by Spalart and Shur,[24] it is an objective form that unifies rotation and curvature. As such, it handles streamline curvature on the basis of Bradshaw's analogy between rotation and curvature.[42] It follows that our model should also mark some improvement in the prediction of strongly curved flows. Future work will involve an assessment of its behavior in complex turbomachinery flows.

ACKNOWLEDGMENT

This work was partially supported by the European Community through the FP5 Project STR (Small Turbomachinery Research).

APPENDIX A: ANALYTICAL SOLUTIONS OBTAINED WITH THE HPB-CORRECTED (k,ϵ) MODEL IN THE HS-Ω FLOW

We suppose that $C_{\mathrm{sc}}>C_{\mathrm{sc1}}$. In this case, both β_1 and β_2 exist; otherwise, the solutions can be immediately deduced from those given here. The evolution equations can be recast in the form

$$\frac{d\alpha}{dt^*}=-a\alpha^2-b,$$

$$\frac{1}{k}\frac{dk}{dt^*}=\frac{C_\mu}{\alpha}-\alpha,$$

$$\frac{1}{\epsilon}\frac{d\epsilon}{dt^*}=\frac{C_\mu-b}{\alpha}-C^0_{\epsilon 2}\alpha,$$

with

$$a=C^0_{\epsilon 2}-1,\quad b=C_{\mathrm{sc}}C^0_{\epsilon 2}\beta(1-2\beta)-C_\mu(C_{\epsilon 1}-1).$$

The first equation can be directly integrated, integration of the k and ϵ equations follows. We remark that a is always positive, and that the sign of b depends on the value of β, leading to consider three different cases.

1. Case 1: $b<0\Leftrightarrow\beta\in\,]-\infty,\beta_1[\cup]\beta_2,\infty[$

The fixed point is given by $\alpha_\infty=\sqrt{-b/a}$. Depending on the initial condition we get the following expressions:

(i) If $\alpha_0>\alpha_\infty$,

$$\frac{\alpha}{\alpha_0}=\frac{\tanh(C_0)}{\tanh(\sqrt{-ab}t^*+C_0)},$$

$$\frac{k}{k_0}=\left[\frac{\cosh(C_0)}{\cosh(\sqrt{-ab}t^*+C_0)}\right]^{C_\mu/b}\times\left[\frac{\sinh(C_0)}{\sinh(\sqrt{-ab}t^*+C_0)}\right]^{1/a},$$

$$\frac{\epsilon}{\epsilon_0}=\left[\frac{\cosh(C_0)}{\cosh(\sqrt{-ab}t^*+C_0)}\right]^{C_\mu/b-1}\times\left[\frac{\sinh(C_0)}{\sinh(\sqrt{-ab}t^*+C_0)}\right]^{C^0_{\epsilon 2}/a}.$$

(ii) If $\alpha_0<\alpha_\infty$,

$$\frac{\alpha}{\alpha_0}=\frac{\tanh\left(\sqrt{-ab}t^*+C_0\right)}{\tanh(C_0)},$$

$$\frac{k}{k_0}=\left[\frac{\sinh(C_0)}{\sinh\left(\sqrt{-ab}t^*+C_0\right)}\right]^{C_\mu/b}\times\left[\frac{\cosh(C_0)}{\cosh\left(\sqrt{-ab}t^*+C_0\right)}\right]^{1/a},$$

$$\frac{\epsilon}{\epsilon_0}=\left[\frac{\sinh(C_0)}{\sinh\left(\sqrt{-ab}t^*+C_0\right)}\right]^{C_\mu/b-1}\times\left[\frac{\cosh(C_0)}{\cosh\left(\sqrt{-ab}t^*+C_0\right)}\right]^{C^0_{\epsilon 2}/a}.$$

(iii) If $\alpha_0=\alpha_\infty$,

$$\frac{\alpha}{\alpha_0}=1,\quad \frac{k}{k_0}=\frac{\epsilon}{\epsilon_0}=\exp\left(\frac{aC_\mu+b}{\sqrt{-ab}}t^*\right),$$

where

$$C_0=\frac{1}{2}\ln\left|\frac{\alpha_\infty+\alpha_0}{\alpha_\infty-\alpha_0}\right|.$$

2. Case 2: $b=0\Leftrightarrow\beta=\beta_1$ or $\beta=\beta_2$

Whatever the initial condition is, we get the following expressions:

$$\frac{\alpha}{\alpha_0}=(1+a\alpha_0t^*)^{-1},$$

$$\frac{k}{k_0}=(1+a\alpha_0t^*)^{-1/a}\exp\left(\frac{C_\mu}{\alpha_0}t^*+aC_\mu\frac{t^{*2}}{2}\right),$$

$$\frac{\epsilon}{\epsilon_0}=(1+a\alpha_0t^*)^{-C^0_{\epsilon 2}/a}\exp\left(\frac{C_\mu}{\alpha_0}t^*+aC_\mu\frac{t^{*2}}{2}\right).$$

The flow is unstable with α going to zero and k and ϵ going to infinity when t^* goes to infinity.

3. Case 3: $b>0\Leftrightarrow\beta\in]\beta_1,\beta_2[$

The equilibrium state does not exist; we get the following expressions:

$$\frac{\alpha}{\alpha_0}=\frac{\tan(C_0)}{\tan(\sqrt{ab}t^*+C_0)},$$

$$\frac{k}{k_0}=\left[\frac{\cos(C_0)}{\cos(\sqrt{ab}t^*+C_0)}\right]^{C_\mu/b}\left[\frac{\sin(C_0)}{\sin(\sqrt{ab}t^*+C_0)}\right]^{1/a},$$

$$\frac{\epsilon}{\epsilon_0}=\left[\frac{\cos(C_0)}{\cos(\sqrt{ab}t^*+C_0)}\right]^{C_\mu/b-1}\times\left[\frac{\sin(C_0)}{\sin(\sqrt{ab}t^*+C_0)}\right]^{C^0_{\epsilon 2}/a},$$

with

$$C_0=\arctan\frac{\sqrt{b/a}}{\alpha_0}.$$

The system develops a blowup at finite time: $t_1^*=(\pi/2-C_0)/\sqrt{ab}$.

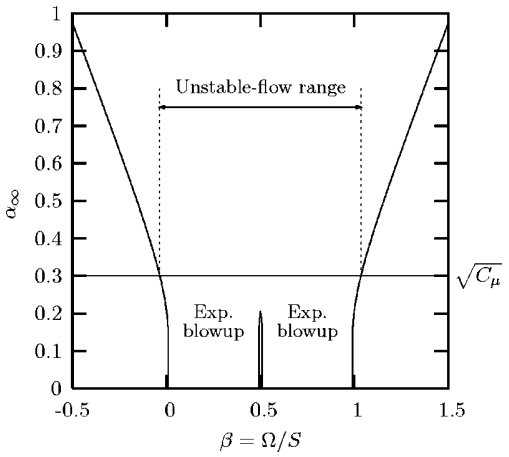

FIG. 9. Fixed-point diagram obtained in the HS-Ω flow with the initial form of Hellsten's correction (Ref. 20).

APPENDIX B: FIXED-POINT DIAGRAM OBTAINED WITH THE INITIAL FORM OF HELLSTEN'S CORRECTION (REF. 20)

The fixed points have been obtained from a numerical solution of Eq. (7). The result is given in Fig. 9. The calculation has been performed with

$$C_\mu=0.09,\quad C_{\epsilon 1}=1.44,\quad C^0_{\epsilon 2}=1.92,\quad C_{\rm sc}=0.4,$$

and

$$C_{\epsilon 2}=C^0_{\epsilon 2}\left[1-C_{\rm sc}\frac{|S-2\Omega|(S-|S-2\Omega|)}{\epsilon^2/k^2}\right]^{-1}$$

The unstable-flow range goes from $\beta\approx-0.035$ to $\beta\approx1.035$ and blowup is expected when $\beta\in]0.09,0.491[\cup]0.509,0.991[$.

[1] D. J. Tritton, "Stabilization and destabilization of turbulent shear flow in a rotating fluid," J. Fluid Mech. **241**, 503 (1992).
[2] J. H. G. Howard, S. V. Patankar, and R. M. Bordynuik, "Flow prediction in rotating ducts using Coriolis-modified turbulence models," ASME Trans. J. Fluids Eng. **102**, 456 (1980).
[3] T. Jongen, L. Machiels, and T. B. Gatski, "Predicting noninertial effects with linear and nonlinear eddy viscosity and algebraic stress models," Flow, Turbul. Combust. **60**, 215 (1998).
[4] R. Kristoffersen and H. I. Andersson, "Direct simulations of low-Reynolds-number turbulent flow in a rotating channel," J. Fluid Mech. **256**, 163 (1993).
[5] E. Lamballais, M. Lesieur, and O. Métais, "Effects of spanwise rotation on the vorticity stretching in transitionnal and turbulent channel flow," Int. J. Heat Fluid Flow **17**, 324 (1996).
[6] C. G. Speziale and N. M. G. Mhuiris, "On the prediction of equilibrium states in homogeneous turbulence," J. Fluid Mech. **209**, 591 (1989).
[7] W. G. Rose, "Results of an attempt to generate a homogeneous turbulent shear flow," J. Fluid Mech. **25**, 577 (1966).
[8] J. J. Rhor, E. C. Itsweire, K. N. Helland, and C. W. V. Atta, "An investigation of the growth of turbulence in a uniform-mean-shear flow," J. Fluid Mech. **187**, 1 (1988).
[9] S. Tavoularis and U. J. Karnik, "Further experiments on the evolution of turbulent stresses and scalars in uniformly sheared turbulence," J. Fluid Mech. **204**, 457 (1989).
[10] R. S. Rogallo, "Numerical experiment in homogeneous turbulence," TM 81315, NASA, 1981.
[11] J. Bardina, J. H. Ferziger, and W. C. Reynolds, "Improved turbulence models based on large-eddy simulation of homogeneous, incompressible turbulent flows," Stanford University, Technical Report No. TF-19, 1983.
[12] J. P. Johnston, R. M. Halleen, and D. K. Lezius, "Effect of spanwise

rotation on the structure of two-dimensional fully developed turbulent channel flow," J. Fluid Mech. **56**, 533 (1972).
[13]D. J. Tritton and P. Davies, "Hydrodynamic instabilities and the transition to turbulence," *Instabilities in Geophysical Fluid Dynamics* (Springer, Heidelberg, 1981), Chap. 8, pp. 229–270.
[14]D. K. Lezius and J. P. Johnston, "Roll-cell instabilities in rotating laminar and turbulent channel flow," J. Fluid Mech. **77**, 153 (1976).
[15]C. Cambon, J.-P. Benoit, L. Shao, and L. Jacquin, "Stability analysis and large-eddy simulation of rotating turbulence with organized eddies," J. Fluid Mech. **278**, 175 (1994).
[16]C. G. Speziale, R. Abid, and G. A. Blaisdell, "On the consistency of Reynolds stress turbulence closures with hydrodynamic stability theory," Phys. Fluids **8**, 781 (1996).
[17]J. P. Bertoglio, "Homogeneous turbulent field within a rotating frame," AIAA J. **20**, 1175 (1982).
[18]C. P. Chen and K. L. Guo, "Low Reynolds number turbulence modeling of rotating flows," *Forum on Turbulent Flows 1990* (ASME, New York, 1990), FED Vol. 94, p. 29.
[19]B. E. Launder, C. H. Priddin, and B. I. Sharma, "The calculation of turbulent boundary layers on spinning and curved surfaces," ASME Trans. J. Fluids Eng. **99**, 231 (1977).
[20]A. Hellsten, "Some improvements in $k-\omega$ SST turbulence model," AIAA Paper 98-2554, 1998, 29th AIAA Fluid Dynamics Conference, 15–18 June 1997, Albuquerque, NM.
[21]D. C. Wilcox, "Reassessment of the scale determining equation for advanced turbulence models," AIAA J. **26**, 1299 (1988).
[22]S. W. Park and M. K. Chung, "Curvature-dependent two-equation model of turbulence for prediction of turbulent recirculation flows," AIAA J. **27**, 340 (1989).
[23]A. Khodak and C. Hirsch, "Second order non-linear $k-\epsilon$ models with explicit effect of curvature and rotation," *Computational Fluid Dynamics '96* (Wiley, New York, 1996), p. 690.
[24]P. R. Spalart and M. Shur, "On the sensitization of turbulence models to rotation and curvature," Aerospace Science and Technology **5**, 297 (1997).
[25]W. P. Jones and B. E. Launder, "The prediction of laminarization with a two-equation model of turbulence," Int. J. Heat Mass Transfer **15**, 301 (1972).
[26]R. A. Wigeland and H. M. Nagib, "Grid generated turbulence with and without rotation about the streamwise direction," Illinois Institute of Technology, Report No. R. 78-1, 1978.
[27]L. Jacquin, O. Leuchter, C. Cambon, and J. Mathieu, "Homogeneous turbulence in the presence of rotation," J. Fluid Mech. **220**, 1 (1990).
[28]J. Bardina, J. H. Ferziger, and R. S. Rogallo, "Effect of rotation on isotropic turbulence: computation and modeling," J. Fluid Mech. **154**, 321 (1985).
[29]K. Dang and P. Roy, "Direct and large eddy simulation of homogeneous turbulence submitted to solid body rotation," *Proceedings of the Fifth Symposium on Turbulent Shear Flows*, Ithaca, Cornell University, 1985.
[30]C. Cambon, J. P. Bertoglio, and D. Jeandel, "Spectral closures for homogeneous turbulence," *The 1980–1981 AFOSR-HTTM, Stanford Conference on Complex Turbulent Flows*, edited by S. J. Kline, B. J. Cantwell, and G. M. Lilley (Stanford University Press, Stanford, 1981), Vol. III, p. 1307.
[31]B. Aupoix, J. Cousteix, and J. Liandrat, "Effect of rotation on isotropic turbulence," Proceedings of Fourth International Symposium on Turbulent Shear Flows, Karlsruhe, 1983.
[32]O. Zeman, "A note on the spectra and decay of rotating homogeneous turbulence," Phys. Fluids **6**, 3221 (1994).
[33]M. Okamoto, "Theoretical turbulence modelling of homogeneous decaying flow in a rotating frame," J. Phys. Soc. Jpn. **64**, 2854 (1995).
[34]Y. Zhou, "A phenomenological treatment of rotating turbulence," Phys. Fluids **7**, 2092 (1995).
[35]V. M. Canuto and M. S. Dubovikov, "A dynamical model for turbulence. V. The effect of rotation," Phys. Fluids **9**, 2132 (1997).
[36]R. Rubinstein and Y. Zhou, "Analytical theory of the destruction terms in dissipation rate transport equations," Phys. Fluids **8**, 3172 (1996).
[37]J. Y. Park and M. K. Chung, "A model for the decay of rotating homogeneous turbulence," Phys. Fluids **11**, 1544 (1999).
[38]S. Thangam, X.-H. Wang, and Y. Zhou, "Development of a turbulence model based on theenergy spectrum for flows involving rotation," Phys. Fluids **11**, 2225 (1999).
[39]M. Ji and P. A. Durbin, "On the equilibrium states predicted by second moment models in rotating, stably stratified homogeneous shear flow," Phys. Fluids **16**, 3540 (2004).
[40]B. E. Launder and B. I. Sharma, "Application of the energy-dissipation model of turbulence to the calculation of flow near a spinning disc," Lett. Heat Mass Transfer **1**, 131 (1974).
[41]C. G. Speziale, B. Younis, R. Rubinstein, and Y. Zhou, "On consistency conditions for rotating turbulent flows," Phys. Fluids **10**, 2108 (1998).
[42]P. Bradshaw, "Effects of streamline curvature on turbulent flows," Agardograph 169, AGARD, 1973.
[43]Y. Shimomura, "Turbulence modeling suggested by system rotation," in *Near-Wall Turbulent Flows*, edited by R. M. C. So, C. G. Speziale, and B. E. Launder (Elsevier Science, Amsterdam, 1993), p. 115.